AIMS Mathematics, 11(3): 8382–8406.
DOI: 10.3934/math.2026344
Received: 13 January 2026
Revised: 16 February 2026
Accepted: 28 February 2026
Published: 30 March 2026

https://www.aimspress.com/journal/Math

Research article

Oncological data applications and risk measures of the heavy-tailed Weibull flexible-G family

Fastel Chipepa[1], **Mahmoud M. Abdelwahab**[2,*], **Wilbert Nkomo**[3] **and Mustafa M. Hasaballah**[4]

[1] Department of Mathematics and Statistical Sciences, Botswana International University of Science and Technology, Palapye, Botswana

[2] Department of Mathematics and Statistics, Faculty of Science, Imam Mohammad Ibn Saud Islamic University (IMSIU), Riyadh 11432, Saudi Arabia

[3] Department of Applied Statistics, Manicaland State University of Applied Sciences, P. Bag 7001, Stair Guthrie Road, Fernhill, Mutare, Zimbabwe

[4] Department of Basic Sciences, Marg Higher Institute of Engineering and Modern Technology, Cairo 11721, Egypt

* **Correspondence:** Email: mmabdelwahab@imamu.edu.sa.

Abstract: We introduce the heavy-tailed Weibull flexible-G (HT-WF-G) family of distributions and derive its fundamental properties, including quantile functions and moments. A maximum likelihood estimation procedure is developed for the parameter inference, with its finite-sample performance and asymptotic properties validated through rigorous Monte Carlo simulation studies. Furthermore, we formulate key actuarial risk metrics including the value at risk (VaR), tail value at risk (TVaR), tail variance (TV), and tail variance premium (TVP) within this flexible framework. The model's practical effectiveness is demonstrated through its application to oncology time-to-event data (lung cancer and acute myeloid leukemia). Empirical results consistently affirm the model's superiority over leading benchmark distributions, as evidenced by significant improvements in the goodness-of-fit criteria, thus establishing the HT-WF-G family as an effective tool for statistical modeling in heavy-tailed and complex survival settings.

Keywords: heavy-tailed-G; Weibull-flexible-G; estimation; Monte Carlo simulations; risk metrics; goodness-of-fit
Mathematics Subject Classification: 62E10, 60E30

1. Introduction

Probability distributions are fundamental to model real-world phenomena across diverse fields including finance, engineering, and medical sciences. Recent advancements in the distribution theory have focused on developing increasingly flexible models to capture complex data behaviors such as skewness, heavy tails, and multimodal patterns. The accurate assessment of tail risk in modern datasets, which often contain extreme outliers, necessitates robust modeling frameworks that surpass traditional distributions including the Pareto, normal, exponential, and Weibull distributions. This need has driven the adoption of advanced generalized and composite models.

A major advancement has been the development of generator techniques to extend existing distributions. Notable frameworks include the following: (1) the T-X family [1], which provides a generalized approach for distribution generation; (2) the Weibull-G generator [2], which introduces enhanced flexibility for lifetime data modeling; and (3) the exponentiated half logistic-G (EHL-G) distribution [3], which offers improved capabilities for skewed data analyses. These generators significantly expand the statistical modeling capabilities through additional shape and scale parameters that enhance the adaptability to diverse real-world scenarios.

Particularly relevant to this study is the type I heavy-tailed-G distribution [4], which has demonstrated a superior performance in modeling heavy-tailed phenomena. Heavy-tailed distributions have gained prominence due to their ability to model extreme events, which is especially crucial in risk assessments, reliability engineering, and actuarial science. Recent works highlighting the growing interest in this area include: the heavy-tailed beta-power transformed Weibull distribution [5], the Topp-Leone type I heavy-tailed-G power series class [6], the heavy-tailed exponential distribution [7], the heavy-tailed log-logistic distribution [8], the type I heavy-tailed odd power generalized Weibull-G family [9], the exponentiated half logistic-type I heavy-tailed-G family [10], the Risti'c-Balakrishnan-heavy-tailed-type II Topp-Leone-G family [11], and the type I heavy-tailed-odd Burr III-G family [12]. These distributions provide robust frameworks to analyze datasets with rare but high-impact events such as financial crashes, catastrophic failures, or extreme survival times.

Building on these advancements, we propose the heavy-tailed Weibull flexible-G (HT-WF-G) family of distributions (FDs), which combines the flexibility of the Weibull flexible-G (WF-G) framework [13] with the heavy-tailed properties introduced in [4]. This new FDs not only generalizes several existing models but also offers an enhanced capability to represent diverse hazard rate shapes including increasing, decreasing, bathtub, and inverted bathtub patterns, thus making it suitable for a wide range of applications.

The paper proceeds as follows: Section 2 introduces the generalized family, detailing its formulation and special cases; Section 3 derives key statistical properties including density expansion, quantile function, and moments; then, the practical aspect of the parameter inference is addressed in Section 4, which outlines the maximum likelihood estimation framework; Section 5 validates the framework's reliability through Monte Carlo simulations across varying sample sizes; a pivotal contribution follows in Section 6, where the model's relevance for AN extreme-value analysis is advanced through the formulation of essential actuarial risk measures, supported by a numerical study to quantify the tail behavior; Section 7 demonstrates the model's superiority through empirical cases, including lung cancer, and acute myeloid leukemia datasets; and finally, Section 8 synthesizes the research contributions and suggests directions for future research.

2. The new family

The new flexible generalized (F-G) FDs [14] has a cumulative distribution function (cdf), which is given by the following:

$$F(z;\Psi) = 1-\bar{G}(z;\Psi)^{-G(z;\Psi)}, \tag{2.1}$$

where $z>0$, and Ψ is a parameter vector from the parent distribution $G(\cdot)=1-\bar{G}(\cdot)$.

A new odd WF-G FDs [13] was developed using the F-G generator. The WF-G FDs generalizes the Weibull-G FDs [15]. The cdf of the WF-G FDs is given by the following:

$$F(z;\alpha,\Psi) = 1-\exp\left\{-\left[\bar{G}(z;\Psi)^{-G(z;\Psi)}-1\right]^{\alpha}\right\}, \tag{2.2}$$

for $z>0$, $\alpha>0$ and, parent parameter vector Ψ.

The heavy-tailed-G (HT-G) FDs [4] with cdf is as follows:

$$F(z;\lambda,\Psi) = 1-\left(\frac{\bar{G}(z;\Psi)}{1-(1-\lambda)G(z;\Psi)}\right)^{\lambda}, \tag{2.3}$$

where $\lambda>0$ is a tilt parameter, $z>0$, and Ψ is the parameter vector from the parent distribution $G(.)$.

By substituting the parent cdf in Eq (2.3) with the WF-G cdf, we obtain the HT-WF-G FDs with cdf given by the following:

$$F(z;\alpha,\lambda,\Psi) = 1-\left(\frac{\exp\left\{-\left[\bar{G}(z;\Psi)^{-G(z;\Psi)}-1\right]^{\alpha}\right\}}{1-(1-\lambda)\left(1-\exp\left\{-\left[\bar{G}(z;\Psi)^{-G(z;\Psi)}-1\right]^{\alpha}\right\}\right)}\right)^{\lambda}, \tag{2.4}$$

for $\alpha,\lambda>0$, and parameter vector Ψ. Through differentiation of Eq (2.4), we obtain the pdf of the HT-WF-G FDs given by the following:

$$\begin{aligned} f(z;\alpha,\lambda,\Psi) &= \lambda^2\alpha g(z;\Psi)\bar{G}(z;\Psi)^{-G(z;\Psi)}\left[\frac{G(z;\Psi)}{\bar{G}(z;\Psi)}-\log\bar{G}(z;\Psi)\right] \\ &\times \left[\bar{G}(z;\Psi)^{-G(z;\Psi)}-1\right]^{\alpha-1}\exp\left\{-\lambda\left[\bar{G}(z;\Psi)^{-G(z;\Psi)}-1\right]^{\alpha}\right\} \\ &\times \left[1-(1-\lambda)\left(1-\exp\left\{-\left[\bar{G}(z;\Psi)^{-G(z;\Psi)}-1\right]^{\alpha}\right\}\right)\right]^{-(\lambda+1)}, \end{aligned} \tag{2.5}$$

for $\alpha,\lambda>0$ and parameter vector Ψ. It is important to note that sub-families of this FDs are obtained by setting the individual parameters of the HT-WF-G FDs to unit. The hazard rate function (hrf) for the HT-WF-G FDs is given by the following:

$$\begin{aligned} h(z;\alpha,\lambda,\Psi) &= \lambda^2\alpha g(z;\Psi)\bar{G}(z;\Psi)^{-G(z;\Psi)}\left[\frac{G(z;\Psi)}{\bar{G}(z;\Psi)}-\log\bar{G}(z;\Psi)\right] \\ &\times \left[1-(1-\lambda)\left(1-\exp\left\{-\left[\bar{G}(z;\Psi)^{-G(z;\Psi)}-1\right]^{\alpha}\right\}\right)\right]^{-1}, \end{aligned} \tag{2.6}$$

for $\alpha,\lambda>0$ and parameter vector Ψ.

2.1. Particular cases

This subsection presents some particular cases of HT-WF-G FDs by specifying $G(z;\Psi)$ and $g(z;\Psi)$ in Eqs (2.4) and (2.5). The Kumaraswamy, Weibull, and Burr XII distributions serve as baseline distributions.

2.1.1. Heavy-tailed-Weibull flexible-Kumaraswamy (HT-WF-Kum) distribution

Considering the Kumaraswamy distribution with the cdf $G(z;\gamma,b) = 1-(1-z^{\gamma})^{b}$ and pdf $g(z;\gamma,b) = \gamma b z^{\gamma-1}(1-z^{\gamma})^{b-1}$ as the baseline distribution, for $\gamma, b, z > 0.$, we have the HT-WF-Kum distribution with cdf

$$F(z;\alpha,\lambda,\gamma,b) = 1-\left(\frac{\exp\{-[Kum_G(z;\gamma,b)-1]^{\alpha}\}}{1-(1-\lambda)(1-\exp\{-[Kum_G(z;\gamma,b)-1]^{\alpha}\})}\right)^{\lambda}$$

and pdf

$$\begin{aligned} f(z;\alpha,\lambda,\gamma,b) &= \lambda^2\alpha\gamma b z^{\gamma-1}(1-z^{\gamma})^{b-1}Kum_G(z;\gamma,b)\left[\frac{1-(1-z^{\gamma})^{b}}{(1-z^{\gamma})^{b}}-\log\left((1-z^{\gamma})^{b}\right)\right][K_G(z;\gamma,b)-1]^{\alpha-1} \\ &\times \exp\{-\lambda[Kum_G(z;\gamma,b)-1]^{\alpha}\}[1-(1-\lambda)(1-\exp\{-[Kum_G(z;\gamma,b)-1]^{\alpha}\})]^{-(\lambda+1)}, \end{aligned}$$

for $\alpha,\lambda,\gamma,b,z>0$, where $Kum_G(z;\gamma,b) = [(1-z^{\gamma})^{b}]^{-[1-(1-z^{\gamma})^{b}]}$. The hrf is as follows:

$$\begin{aligned} h(z;\alpha,\lambda,\gamma,b) &= \lambda^2\alpha\gamma b z^{\gamma-1}(1-z^{\gamma})^{b-1}Kum_G(z;\gamma,b)\left[\frac{1-(1-z^{\gamma})^{b}}{(1-z^{\gamma})^{b}}-\log\left((1-z^{\gamma})^{b}\right)\right][Kum_G(z;\gamma,b)-1]^{\alpha-1} \\ &\times [1-(1-\lambda)(1-\exp\{-[KumK_G(z;\gamma,b)-1]^{\alpha}\})]^{-1}. \end{aligned}$$

In Figure 1(a), the distribution demonstrates considerable flexibility in its density profiles, thereby encompassing unimodal forms with varying peak locations and sharpness, as well as bimodal and multimodal configurations contingent upon parameter choices. Additionally, it can capture both symmetric and asymmetric distributional shapes. The hrf plot in Figure 1(b) further underscores the model's adaptability, thereby revealing its capacity to represent a wide spectrum of failure patterns, such as bathtub-shaped, upside-down bathtub, monotonically increasing, and monotonically decreasing hazard rates.

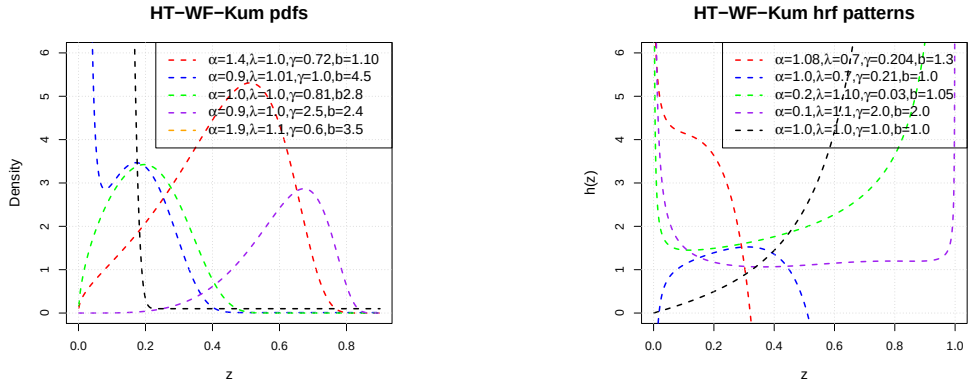

(a) pdf plots **(b)** hrf plots

Figure 1. Plots of pdf and hrf for the HT-WF-Kum distribution.

Figure 2 presents the HT-WF-Kum distribution's shape flexibility through 3D and contour analyses under fixed α and b, by varying λ and γ parameters. The study demonstrates the model's exceptional flexibility in kurtosis, where synergistic parameter interactions produce a nonlinear increase, thus allowing precise tail behavior modulation. Additionally, the distribution exhibits a wide skewness range, thereby transitioning from left to right asymmetry along a diagonal boundary in the λ-γ plane, the enabling accurate modeling of the diverse asymmetry patterns.

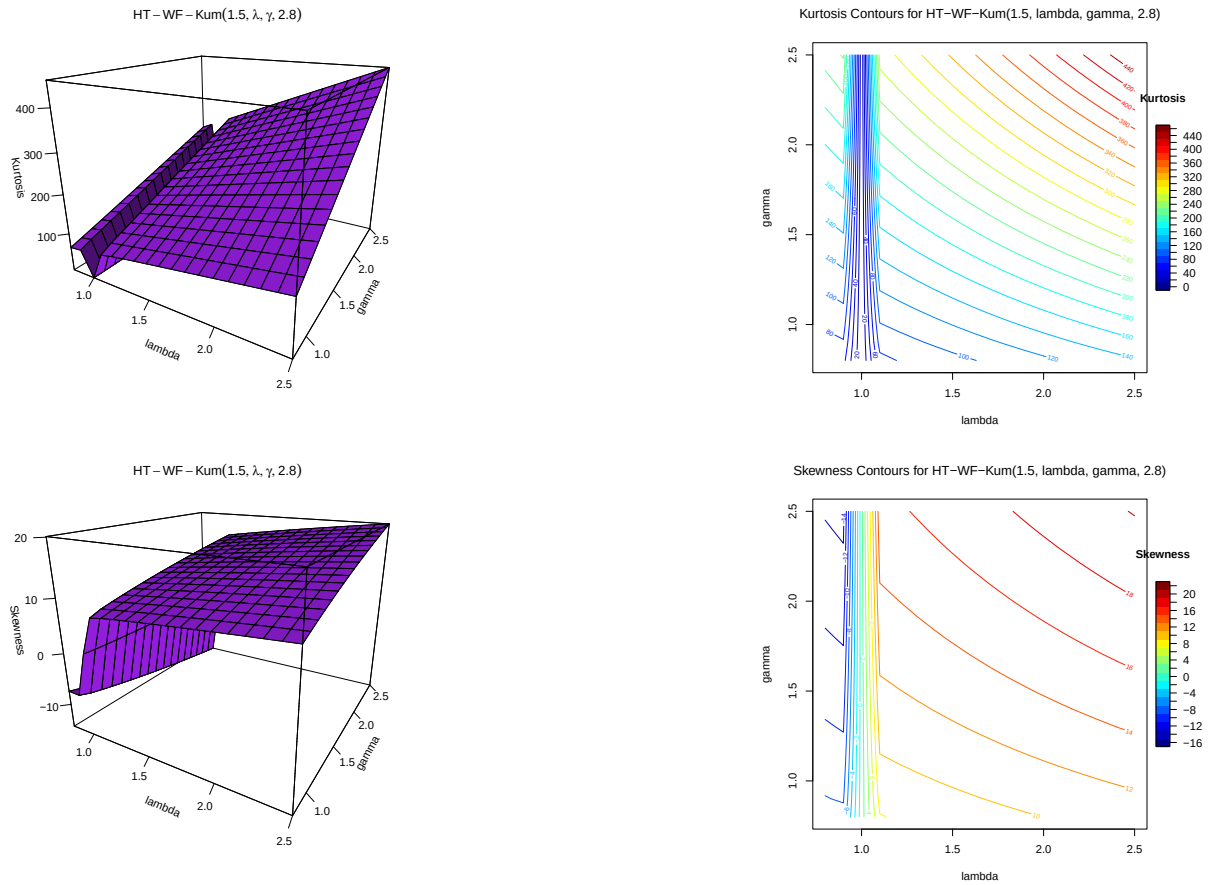

Figure 2. HT-WF-Kum kurtosis and skewness plots for selected parameter values.

2.1.2. Heavy-tailed-Weibull flexible-Weibull (HT-WF-W) distribution

The Weibull distribution has cdf $G(z; c, \omega) = 1 - \exp(-cz^{\omega})$, and pdf $g(z; c, \omega) = c\omega z^{\omega-1} \exp(-cz^{\omega})$, for $c, \omega, z > 0$. If the Weibull distribution is used as the baseline distribution for the HT-WF-G distribution as the baseline, then we have the HT-WF-W distribution with cdf

$$F(z; \alpha, \lambda, c, \omega) = 1 - \left(\frac{\exp\left\{-\left[[\exp(-cz^{\omega})]^{-[1-\exp(-cz^{\omega})]} - 1\right]^{\alpha}\right\}}{1 - (1-\lambda)\left(1 - \exp\left\{-\left[[\exp(-cz^{\omega})]^{-[1-\exp(-cz^{\omega})]} - 1\right]^{\alpha}\right\}\right)} \right)^{\lambda}$$

and pdf

$$f(z;\alpha,\lambda,c,\omega) = \lambda^2\alpha c\omega z^{\omega-1}[\exp(-cz^{\omega}]^{[\exp(-cz^{\omega})]}\left[\frac{1-\exp(-cz^{\omega})}{\exp(-cz^{\omega})} - \log\left(\exp(-cz^{\omega})\right)\right][W_G(z;c,\omega)-1]^{\alpha-1}$$
$$\times \exp\left\{-\lambda\left[W_G(z;c,\omega)-1\right]^{\alpha}\right\}\left[1-(1-\lambda)\left(1-\exp\left\{-\left[W_G(z;c,\omega)-1\right]^{\alpha}\right\}\right)\right]^{-(\lambda+1)},$$

for $\alpha, \lambda, c, \omega, z > 0$, where $W_G(z;c,\omega) = \exp(-cz^{\omega}))[\exp(-cz^{\omega}]^{-[1-\exp(-cz^{\omega})]}$. The hrf is as follows:

$$h(\alpha,\lambda,c,\omega) = \lambda^2\alpha c\omega z^{\omega-1}[\exp(-cz^{\omega}]^{[\exp(-cz^{\omega})]}\left[\frac{1-\exp(-cz^{\omega})}{\exp(-cz^{\omega})} - \log\left(\exp(-cz^{\omega})\right)\right][W_G(z;c,\omega)-1]^{\alpha-1}$$
$$\times \left[1-(1-\lambda)\left(1-\exp\left\{-\left[W_G(z;c,\omega)-1\right]^{\alpha}\right\}\right)\right]^{-1}.$$

The density plots in Figure 3 demonstrate the adaptability of the HT-WF-W distribution in accommodating diverse datasets, including those that are positively skewed, negatively skewed, nearly symmetric, J shaped, and reversed-J shaped. Similarly, the hrf plot demonstrates its effectiveness in capturing patterns such as decreasing, increasing, and inverted bathtub patterns.

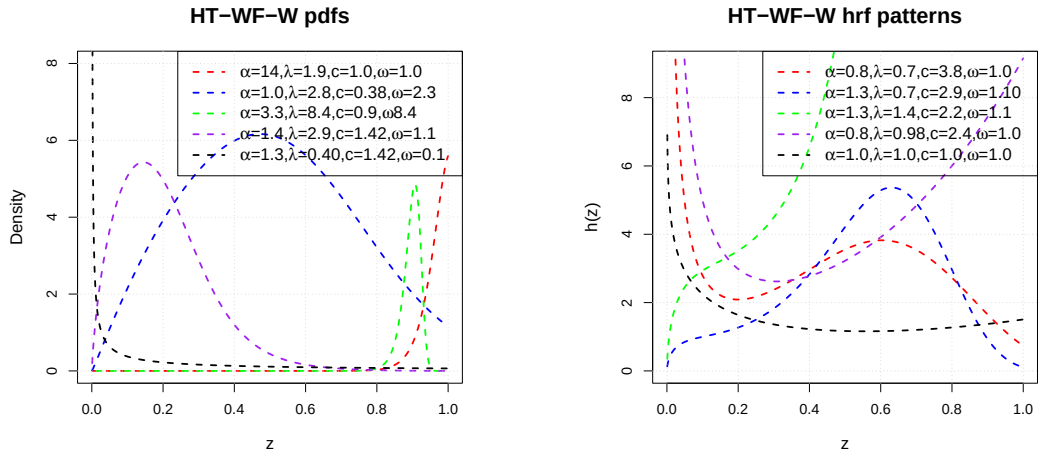

(a) pdf plots **(b)** hrf plots

Figure 3. Plots showing the pdf and hrf for the HT-WF-W distribution.

In Figure 4, a set of 3D and contour plots illustrates the variability in skewness and kurtosis characteristics of the HT-WF-W distribution. The kurtosis exhibits significant flexibility, indicating that the distribution can model both moderate and extreme tail heaviness. Kurtosis decreases as α and ω increase. Additionally, the skewness of the HT-WF-W distribution varies flexibly with parameters α and ω. As α increases, skewness decreases, while an increasing ω enhances the skewness, thereby extending the tail. The distribution exhibits a range of positive skewness values, indicating its adaptability to different asymmetric data shapes.

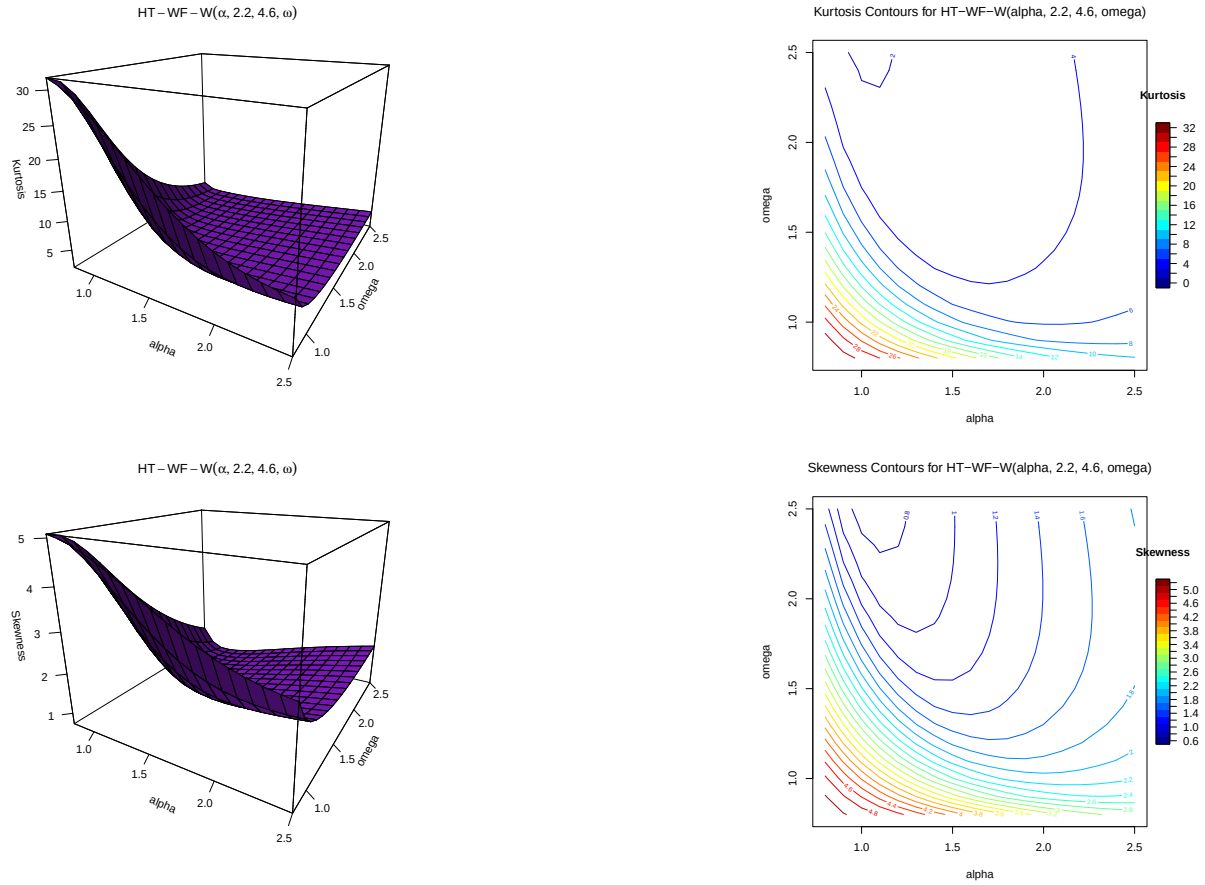

Figure 4. HT-WF-W distribution's kurtosis and skewness plots for selected parameters.

2.1.3. Heavy-tailed-Weibull flexible-Burr XII (HT-WF-BXII) distribution

The Burr XII distribution is defined by the cdf $G(z;\beta,k) = 1-(1+z^{\beta})^{-k}$ and pdf $g(z;\beta,k) = \frac{\beta k z^{\beta-1}}{(1+z^{\beta})^{k+1}}$, where $z,\beta,k > 0$. Employing the Burr XII pioneered by Burr [16] as the baseline distribution to the HT-WF-G FDs yields the HT-WF-BXII. The HT-WF-BXII distribution has the cdf

$$F(z;\alpha,\lambda,\beta,k) = 1-\left(\frac{\exp\{-[B_G(z;\beta,k)-1]^{\alpha}\}}{1-(1-\lambda)(1-\exp\{-[B_G(z;\beta,k)-1]^{\alpha}\})}\right)^{\lambda},$$

and pdf

$$\begin{aligned} f(z;\alpha,\lambda,\beta,k) &= \frac{\lambda^2\alpha\beta k z^{\beta-1}}{(1+z^{\beta})^{k+1}}B_G(z;\beta,k)\left[\frac{1-(1+z^{\beta})^{-k}}{(1+z^{\beta})^{-k}}-\log[(1+z^{\beta})^{-k}]\right][B_G(z;\beta,k)-1]^{\alpha-1} \\ &\times \exp\{-\lambda[B_G(z;\beta,k)-1]^{\alpha}\}[1-(1-\lambda)(1-\exp\{-[B_G(z;\beta,k)-1]^{\alpha}\})]^{-(\lambda+1)}, \end{aligned}$$

for $\alpha,\lambda,\beta,k,z > 0$, where $B_G(z;\beta,k) = [(1+z^{\beta})^{-k}]^{-[1-(1+z^{\beta})^{-k}]}$. The hrf is as follows:

$$\begin{aligned} h(z;\alpha,\lambda,\beta,k) &= \frac{\lambda^2\alpha\beta k z^{\beta-1}}{(1+z^{\beta})^{k+1}}B_G(z;\beta,k)\left[\frac{1-(1+z^{\beta})^{-k}}{(1+z^{\beta})^{-k}}-\log[(1+z^{\beta})^{-k}]\right][B_G(z;\beta,k)-1]^{\alpha-1} \\ &\times [1-(1-\lambda)(1-\exp\{-[B_G(z;\beta,k)-1]^{\alpha}\})]^{-1}. \end{aligned}$$

A particularly compelling feature of the HT-WF-BXII distribution is its ability to generate special distributions through parameter simplification. Specifically, when $k = 1$, the heavy-tailed-Weibull flexible-log-logistic (HT-WF-LLoG) distribution emerges as a special case, while setting $\beta = 1$ yields the heavy-tailed-Weibull flexible-Lomax (HT-WF-Lom) distribution. These derivations elegantly demonstrate the flexibility of the HT-WF-G framework, thereby enabling tailored modeling for distinct data behaviors and expanding its applicability to diverse statistical scenarios.

The density plots in Figure 5 illustrate the HT-WF-BXII distribution's capacity to model a broad spectrum of data configurations, including positively skewed, negatively skewed, approximately symmetric, J shaped, and reversed-J-shaped probability structures. This highlights its robust flexibility for empirical applications. The hrf plots exhibit its dynamic adaptability in characterizing complex failure rate behaviors, such as monotonically decreasing, monotonically increasing, bathtub, and inverted bathtub shapes.

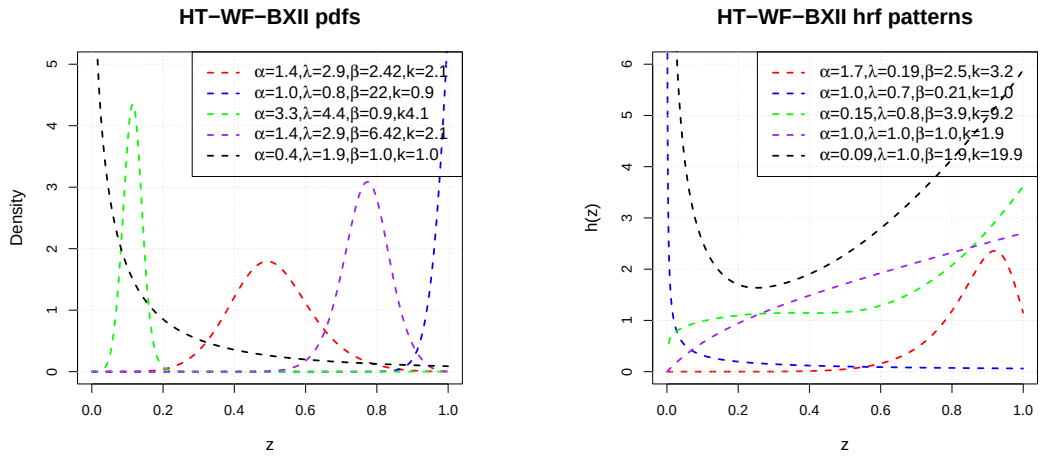

(a) pdf plots **(b)** hrf plots

Figure 5. Density and hrf plots for the HT-WF-BXII distribution.

Figure 6 provides a joint analysis of skewness and kurtosis for the HT-WF-BXII distribution through 3D and contour plots. The analysis, conducted with fixed values of λ and k, reveals a consistent trend: both kurtosis and skewness exhibit a decreasing relationship with the parameters α and β. Specifically, higher values of α and β correspond to a reduction in the kurtosis, thus indicating lighter tails. Similarly, increasing these parameters also leads to a decrease in skewness, resulting in a more symmetrical distribution.

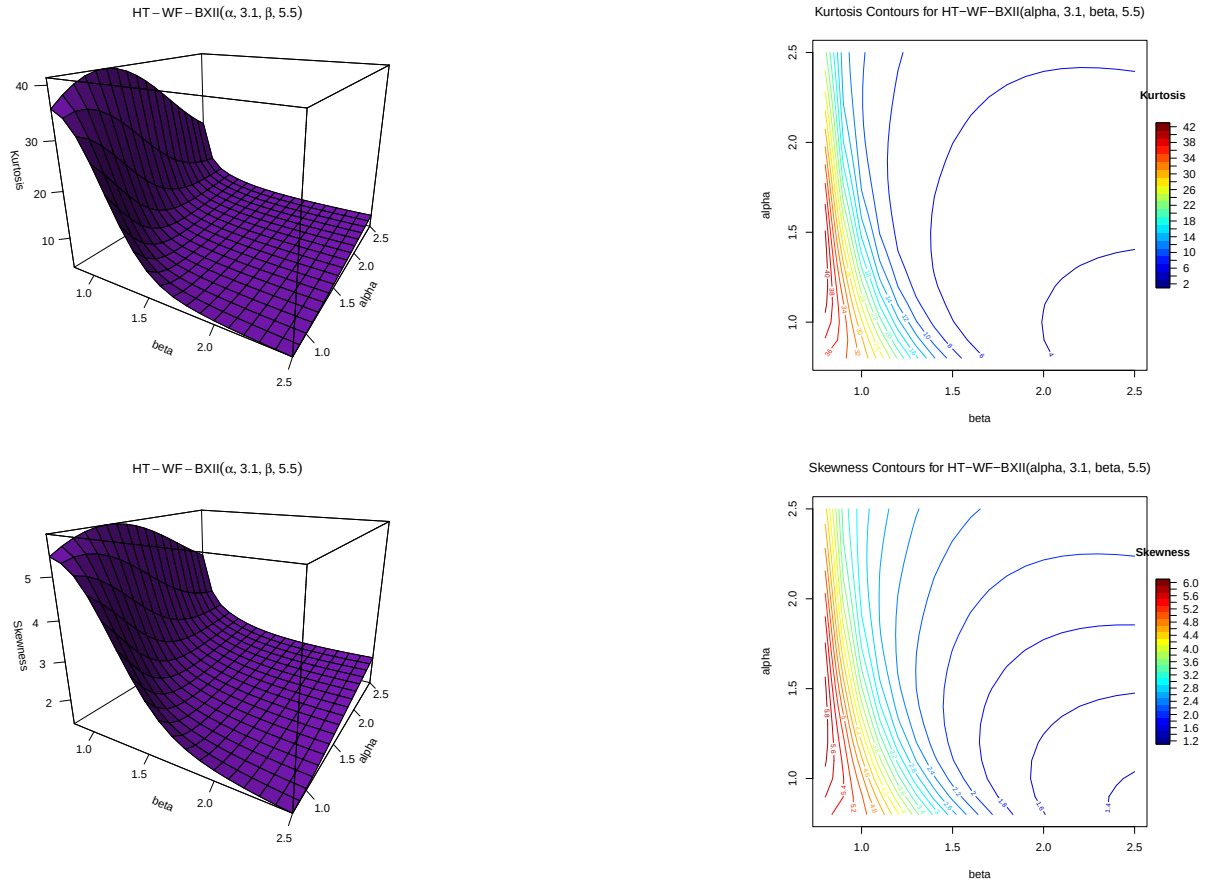

Figure 6. Kurtosis and skewness plots for the HT-WF-BXII distribution.

3. Statistical properties

A series expansion of the density function provides powerful techniques to approximate, estimate, and compute complex distributions. Additionally, statistical properties such as the quantile function (QF), moments, moment generating functions (mgfs), and incomplete moments are fundamental tools to characterize, analyze, and compare probability distributions.

3.1. Quantile function

The quantile function is obtained by inverting the cdf given in Eq (2.4) so that

$$\bar{G}(z;\Psi)^{-G(z;\Psi)} = 1 + \left[-\ln\left(\frac{\lambda(1-u)^{1/\lambda}}{1-(1-\lambda)(1-u)^{1/\lambda}}\right)\right]^{1/\alpha}.$$

Consequently, the quantiles can be obtained from the following:

$$Q_Z(u) = G^{-1}\left[1-\exp\left(W\left(1;\ \ln\left[1+\left(-\ln\frac{\lambda(1-u)^{1/\lambda}}{1-(1-\lambda)(1-u)^{1/\lambda}}\right)^{1/\alpha}\right]\right)\right)\right], \tag{3.1}$$

where $W(a;b)$ is the generalized Lambert W function satisfying $We^W = aW + b$ for a specified baseline $G(.)$ and $u \in [0,1]$.

3.2. Density expansion

Using the series expansions $(1-y)^{-n} = \sum_{j=0}^{\infty}\binom{n+j-1}{j}y^j$ and $(1-y)^n = \sum_{i=0}^{\infty}(-1)^i\binom{n}{i}y^i$, and $e^{-z} = \sum_{l=0}^{\infty}\frac{(-z)^l}{l!}$, we get the following:

$$F(z;\alpha,\lambda,\Psi) = 1-\sum_{i,j,l=0}^{\infty}\binom{n+j-1}{j}(1-\lambda)^j(-1)^i\binom{n}{i}\frac{(-(\lambda+i)^l)}{l!}\left[\bar{G}(z;\Psi)^{-G(z;\Psi)}-1\right]^{\alpha l}.$$

For $0 \le y < 1$, we define a convergent power series (PS) as follows:

$$p(y) = (1-y)^{-y}-1 = y^2\sum_{k=0}^{\infty}\xi_k y^k,$$

where $\xi_0 = 1, \xi_1 = 1/2, \xi_2 = 5/6, \xi_3 = 3/4$, etc. Applying the PS raised to a positive integer

$$\begin{aligned}\left[\bar{G}(z;\Psi)^{-G(z;\Psi)}-1\right]^{\alpha l} &= G^2(z;\Psi)\sum_{k=0}^{\infty}\xi_k G^k(z;\Psi)\\ &= G^{2\alpha l}(z;\Psi)\sum_{k=0}^{\infty}\Theta_k G^k(z;\Psi),\end{aligned}$$

where

$$\Theta_k = \Theta_{\alpha l} = \begin{cases} 1, & k=0\\ \frac{1}{k}\sum_{h=0}^{k-1}[k\alpha l - h(\alpha l+1)]\phi_m\Theta_{k-h}, & k>0.\end{cases}$$

Therefore, we have the following:

$$F(z;\alpha,\lambda,\Psi) = 1-\sum_{i,j,l,k=0}^{\infty}\binom{n+j-1}{j}(1-\lambda)^j(-1)^i\binom{n}{i}\frac{(-(\lambda+i)^l)}{l!}\Theta_{\alpha l}G^{2\alpha l+k}(z;\Psi).$$

Differentiating Eq (3.2), we get the following:

$$\begin{aligned}f(z;\alpha,\lambda,\Psi) &= 1-\sum_{i,j,l,k=0}^{\infty}\binom{n+j-1}{j}(1-\lambda)^j(-1)^i\binom{n}{i}\frac{(-(\lambda+i)^l)}{l!}\Theta_{\alpha l}(2\alpha l+k)g(z;\Psi)G^{2\alpha l+k-1}(z;\Psi)\\ &= \sum_{i,j,l,k=0}^{\infty}\eta_{i,j,l,k}g_{2\alpha l+k}(z;\Psi),\end{aligned} \tag{3.2}$$

where $g_{2\alpha l+k}(z;\Psi)$ is an exponentiated-G (exp-G), with parameter $(2\alpha l+k)$ and, $\eta_{i,j,l,k}$ is the linear component. The infinite series expansion of the density given in Eq (3.2) absolutely converges for all $z > 0$ provided that $\alpha > 0$, $\lambda > 0$, and the baseline survival function satisfies $0 < \bar{G}(z;\Psi) < 1$.

3.3. Moments and incomplete moments

Moments including the mean, variance, skewness, and kurtosis quantify a distribution's central tendency, dispersion, asymmetry, and tail behavior, respectively. Additionally, they are useful in

parameter estimation, hypothesis testing, and comparative analyses across distributions in fields such as engineering and physics. Let $f(z;\alpha,\lambda,\Psi)$ be denoted by $f(z)$. Suppose $W_{2\alpha l+k}$ represents an exp-G distributed random variable with a power parameter $(2\alpha l + k)$; then, the r^{th} moment of the HT-WF-G FDs can be expressed as follows:

$$E\left(Z^r\right) = \int_{-\infty}^{\infty} z^r f(z)dz = \sum_{i,j,l,k=0}^{\infty} \eta_{i,j,l,k} E(W_{2\alpha l+k}^r),$$

where $E(W_{2\alpha l+k}^r)$ represents the r^{th} moment of $W_{2\alpha l+k}$, and $\eta_{i,j,l,k}$ is defined in Eq (3.2). The r^{th} moment $E(Z^r)$ of the HT-WF-G distribution exists and is finite if and only if the corresponding moment exists for the exponentiated baseline variable $W_{2\alpha l+k}$ for all $l,k \geq 0$ in the sum. For a baseline distribution $G(z;\Psi)$ whose survival function decays as $\bar{G}(z;\Psi) \sim z^{-\nu}$ as $z \to \infty$, a sufficient condition for the existence of $E(Z^r)$ is $r < \nu \cdot \min(\alpha,\lambda)$.

The r^{th} incomplete moment can be derived as follows:

$$I_Z(t) = \int_0^t z^r f(z)dz = \sum_{i,j,l,k=0}^{\infty} \eta_{i,j,l,k} I_{2\alpha l+k1}(t;r,\Psi),$$

where $I_{2\alpha l+k1}(t;r,\Psi) = \int_0^t z^r g_{2\alpha l+k}(z;\Psi)dz$ defines the incomplete moment of $W_{2\alpha l+k1}$. Additionally, the mgf of Z is

$$M_Z(t) \quad = \quad \sum_{i,j,l,k=0}^{\infty} \eta_{i,j,l,k} E(e^{tW_{2\alpha l+k1}}),$$

with $E(e^{tW_{2\alpha l+k1}})$ representing the mgf of $W_{2\alpha l+k}$, and $\eta_{i,j,l,k}$ is specified in Eq (3.2). The derivation of incomplete moments is integral to the formulation of Bonferroni and Lorenz curves, which serve as foundational instruments to examine the income disparity, social welfare, and financial risk across diverse disciplines.

(1) **Moment existence:** The r-th moment $E(Z^r)$ of the HT-WF-G distribution exists and is finite if and only if the corresponding moment exists for the exponentiated baseline variable $W_{2\alpha l+k}$ for all $l,k \geq 0$ in the sum. For a baseline distribution $G(z;\Psi)$ whose survival function decays as $\bar{G}(z;\Psi) \sim z^{-\nu}$ as $z \to \infty$, a sufficient condition for the existence of $E(Z^r)$ is $r < \nu \cdot \min(\alpha,\lambda)$.
In practice, the finiteness of moments depends on the tail behavior of G and the parameters α and λ; users should verify the moment existence for their specific baseline choice.

(2) **Series convergence:** The infinite series expansion of the density given in Eq (3.2) absolutely converges for all $z > 0$ provided that $\alpha > 0$, $\lambda > 0$, and the baseline survival function satisfies $0 < \bar{G}(z;\Psi) < 1$. Convergence follows from the fact that the coefficients $\eta_{i,j,l,k}$ decay sufficiently fast; a sufficient condition is that $\lambda < 1$ and the series $\sum \eta_{i,j,l,k}$ is absolutely summable, which holds under mild restrictions on G.

4. Maximum likelihood estimation

Let $z_1, ..., z_n$ be a set of observations from the HT-WF-G distribution given by Eq (2.5). The total log-likelihood function for $\Delta = (\alpha,\lambda,\Psi)^T$ is given by the following:

$$\begin{aligned}
\ell = \ell(\Delta) &= \sum_{i=1}^{n} \log\left(f(z_i;\alpha,\lambda,\Psi)\right) \\
&= n\log\lambda^2\alpha + \sum_{i=1}^{n}\log\left(g(z_i;\Psi)\right) - \sum_{i=1}^{n}\left[-G(z_i;\Psi)\log\bar{G}(z_i;\Psi)\right] + \sum_{i=1}^{n}\log\left[\frac{G(z_i;\Psi)}{\bar{G}(z_i;\Psi)} - \log\bar{G}(z_i;\Psi)\right] \\
&+ (\alpha-1)\sum_{i=1}^{n}\log\left[\bar{G}(z_i;\Psi)^{-G(z_i;\Psi)} - 1\right] - \lambda\sum_{i=1}^{n}\left[\bar{G}(z_i;\Psi)^{-G(z_i;\Psi)} - 1\right]^{\alpha} \\
&- (\lambda+1)\sum_{i=1}^{n}\log\left[1-(1-\lambda)\left(1-\exp\left\{-\left[-G(z_i;\Psi)^{-G(z_i;\Psi)} - 1\right]^{\alpha}\right\}\right)\right]. \qquad (4.1)
\end{aligned}$$

We estimated the maximum likelihood estimation (MLE) by maximizing Eq (4.1) using the optim function and the maxLik library [17] in R (v4.1.1).

5. Simulation study

We conducted a simulation study to evaluate the efficiency of maximum likelihood estimates. The simulation study results are shown in Table 1. We set the parameter $\lambda = 1$ in the HT-WF-BXII pdf. A simulation study was conducted for sample sizes n= 20, 40, 80, 160, 360, and 720 for N=1000 repetitions from the HT-WF-BXII distribution. The average bias (AB) and root mean square error (RMSE) for an estimated parameter, say $(\hat{\alpha})$, is calculated using the following formulae:

$$AB(\hat{\alpha}) = \frac{\sum_{i=1}^{N}\hat{\alpha}_i}{N} - \alpha, \quad \text{and} \quad RMSE(\hat{\alpha}) = \sqrt{\frac{\sum_{i=1}^{N}(\hat{\alpha}_i-\alpha)^2}{N}},$$

Table 1. Monte Carlo simulation results for the HT-WF-BXII distribution: mean, RMSE, and AB.

		$\alpha=0.9,\beta=1.1,k=0.5$			$\alpha=0.8,\beta=0.8,k=0.75$		
	n	Mean	RMSE	AB	Mean	RMSE	AB
	20	2.0261	3.8281	1.1261	3.0635	6.4149	2.2635
	40	1.9384	3.4930	1.0384	2.4853	5.9550	1.6853
	80	1.0524	0.7404	0.1524	1.1474	1.6356	0.3474
α	160	0.9250	0.1750	0.0250	0.8894	0.4768	0.0894
	360	0.9124	0.0932	0.0124	0.8270	0.1619	0.0270
	720	0.9067	0.0722	0.0067	0.8148	0.1101	0.0148
	20	1.4225	1.3767	0.3225	0.9849	1.2344	0.1849
	40	1.2305	0.9671	0.1305	0.9320	0.6106	0.1320
	80	1.1590	0.4413	0.0590	0.8426	0.3813	0.0426
β	160	1.1445	0.3673	0.0445	0.8069	0.2433	0.0069
	360	1.1279	0.1732	0.0021	0.7930	0.1567	-0.0070
	720	1.1013	0.1401	0.0013	0.7998	0.1312	-0.0002
	20	0.6087	0.3540	0.1087	0.8705	0.3596	0.1205
	40	0.6004	0.3482	0.1004	0.7863	0.3150	0.0363
	80	0.5131	0.1813	0.0131	0.7721	0.2096	0.0221
k	160	0.5011	0.1105	0.0011	0.7635	0.1445	0.0135
	360	0.5006	0.0638	0.0006	0.7572	0.0858	0.0072
	720	0.4963	0.0476	-0.0037	0.7497	0.0675	-0.0003

respectively. The results in Table 1 demonstrate that the mean values approximate the true parameter values, and the RMSE and bias decrease toward zero for all parameters as the sample size increases. This implies that the HT-WF-BXII distribution generates consistent parameter estimates.

6. Risk measures

Risk measures are statistical tools utilized by actuaries to assess the market risk. This section focuses on some of the key risk measures.

6.1. Value at risk

The value at risk (VaR) measures the potential financial losses that a firm, portfolio, or position may experience within a defined time period. Note that VaR_u equates to the quantile function; hence, VaR_u for the HT-WF-G FDs is calculated from the following:

$$VaR_u = G^{-1}\left[1-\exp\left(W\left(1;\ \ln\left[1+\left(-\ln\frac{\lambda(1-u)^{1/\lambda}}{1-(1-\lambda)(1-u)^{1/\lambda}}\right)^{1/\alpha}\right]\right)\right)\right], \tag{6.1}$$

where $u \in (0,1)$ represents the significance level, $G(.)$ is the baseline cdf, and $W(a;b)$ is the generalized Lambert W function.

6.2. Tail value at risk

The tail Value at Risk ($TVaR_u$) quantifies the anticipated magnitude of losses in the scenario where an outcome materializes that surpasses a predetermined probability threshold. The $TVaR_u$ for the HT-WF-G FDs is as follows:

$$\begin{aligned} TVaR_u &= E\left(Z|Z>z_u\right) = \frac{1}{1-u}\int_{VaR_u}^{\infty} zf(z)dz \\ &= \frac{1}{1-u}\sum_{i,j,l,k=0}^{\infty}\int_{VaR_u}^{\infty} z\eta_{i,j,l,k}g_{2\alpha l+k}(z;\Psi)dz, \end{aligned} \tag{6.2}$$

where $\eta_{i,j,l,k}$ is as given in Eq (3.2), and $g_{2\alpha l+k}(z;\Psi)$ is the exp-G with parameter $(2\alpha l+k)$.

6.3. Tail variance

The tail Variance (TV_u) measures the conditional variance of losses under the assumption that they exceed the VaR with a specified probability threshold. For the HT-WF-G FDs, the expression for TV_u is as follows:

$$\begin{aligned} TV_u &= E\left(Z^2 \mid Z>z_u\right) - (TVaR)^2 \\ &= \frac{1}{1-u}\int_{VaR_u}^{\infty} z^2 f(z)dz - (TVaR_u)^2 \\ &= \frac{1}{1-u}\sum_{i,j,l,k=0}^{\infty}\eta_{i,j,l,k}\int_{VaR_u}^{\infty} z^2 g_{2\alpha l+k}(z;\Psi)dz - (TVaR_u)^2. \end{aligned} \tag{6.3}$$

Hence, the TV_u of the HT-WF-G FDs can be derived from those of the exp-G distribution.

6.4. Tail variance premium

Risk professionals are focused on situations where risks surpass specific thresholds. These scenarios frequently occur in insurance, particularly in policies that include deductibles and reinsurance agreements. The tail variance premium ($TVaP_u$) addresses these needs. The ($TVaP_u$) of the HT-WF-G FDs is expressed as follows:

$$TVaP_u = TVaR_u + \zeta(TV_u), \tag{6.4}$$

for $0 < \zeta < 1$. The ($TVaP_u$) of the HT-WF-G FDs is found by incorporating $TVaR_u$ and TV_u into Eq (6.4).

6.5. Numerical study

In this subsection, we present an analysis that utilizes numerical simulations to assess the VaR, TVaR, TV, and TVP as risk measures. The risk measures of the HT-WF-BXII distribution are compared to those of the TIHT-W distribution [4], OEHL-BXII distribution [18], and the BXII distribution [16]. The simulation results are obtained by randomly generating samples of size 100 from the specified distributions and estimating the parameters using the ML estimation technique to ensure accurate estimations across different distributions. The calculations are iteratively performed 1000 times to enhance the precision in the estimations across the various distributions.

Table 2 presents the outcomes of numerical simulations carried out to assess the risk measures for the selected four distributions. A model that exhibits higher risk measure values indicates a more significant heavy-tail. Therefore, we can confidently conclude that the HT-WF-BXII distribution has a heavier tail compared to the contending distributions. Consequently, the HT-WF-BXII distribution is well-suited to model heavy-tailed data.

Table 2. Numerical simulation results for risk measures.

Significance level	Risk measure	0.75	0.80	0.85	0.90	0.95	0.99
HT-WF-BXII($\alpha = 0.2, \lambda = 0.1, \beta = 0.3, k = 0.2$)	VaR	17.922	21.929	27.398	35.627	50.939	91.504
	TVaR	20.379	24.888	32.113	45.785	83.143	321.816
	TV	3566.9	4346.7	5563.8	7721.2	12358.2	10356.5
	TVP	2873.9	3502.2	4483.1	6222.7	9969.7	11324.7
TI-HT-W($\theta = 0.5, \lambda = 0.1, \gamma = 1.5$)	VaR	1.10	1.72	2.81	4.99	10.93	39.29
	TVaR	9.20	11.15	14.13	19.32	31.27	77.91
	TV	374.34	448.84	562.89	763.45	1238.58	3257.37
	TVP	308.67	370.23	464.45	630.08	1022.13	2683.80
OEHL-BXII($\alpha = 2.0, \lambda = 1.0, \beta = 0.3, k = 0.2$)	VaR	5.76	7.79	10.48	18.96	21.04	23.19
	TVaR	15.62	16.51	17.10	19.43	26.15	31.21
	TV	190.20	219.12	245.20	267.3	288.4	312.40
	TVP	415.81	452.01	462.90	556.3	666.91	765.12
BXII ($\beta = 0.3, k = 0.2$)	VaR	0.87	1.36	2.21	3.95	8.67	31.31
	TVaR	7.32	8.87	11.24	15.38	24.92	62.24
	TV	239.55	287.34	360.53	489.34	794.84	2095.73
	TVP	198.95	238.74	299.66	406.85	660.80	1738.82

7. Applications

This section presents an empirical evaluation of the HT-WF-BXII distribution to justify the utility of the proposed FDs. We conduct a comparative analysis against competing heavy-tailed distributions that extend the Burr and Weibull distributions, including the following:

- The Topp-Leone Odd Burr III log-logistic Weibull (TL-OBIII-LLOG) [19] with pdf

$$\begin{aligned} f(w;\alpha,\beta,b,\lambda) &= 2\alpha\beta b\left\{1-\left(1-\left[1+\left(\frac{1-(1+w^{\lambda})^{-1}}{1+w^{\lambda})^{-1}}\right)^{-\alpha}\right]^{-\beta}\right)^{2}\right\}^{b-1}\left(1-\left[1+\left(\frac{1-(1+w^{\lambda})^{-1}}{1+w^{\lambda})^{-1}}\right)^{-\alpha}\right]^{-\beta}\right) \\ &\times \frac{\lambda w^{\lambda-1}(1+w^{\lambda})^{-2}}{(1+w^{\lambda})^{-1}}\left[1+\left(\frac{1-(1+w^{\lambda})^{-1}}{1+w^{\lambda})^{-1}}\right)^{-\alpha}\right]^{-\beta-1}\left(\frac{1-(1+w^{\lambda})^{-1}}{1+w^{\lambda})^{-1}}\right)^{-\alpha-1}, \end{aligned}$$

  where $\alpha,\beta,b,\lambda>0$, and $w>0$.
- The type I heavy-tailed Weibull distribution (TI-HT-W) [4], with the pdf

$$f_{TIHT-W}(x;\alpha,\lambda,\gamma) = \frac{\alpha\lambda^{2}\gamma x^{\alpha-1}\exp(-\lambda\gamma x^{\alpha})}{\left[1-(1-\lambda)\left(1-\exp-\gamma x^{\alpha}\right)\right]^{\lambda+1}},$$

  where $\alpha,\lambda,\gamma>0$ and $x>0$.
- The odd exponentiated half logistic Burr XII (OEHL-BXII) [18] whose pdf is as follows:

$$\begin{aligned} f_{OEHLBXII}(x;\alpha,\lambda,\beta,k) &= 2\alpha\lambda\beta k x^{\beta-1}\exp\lambda[1-(1+x^{\beta})^{k}] \\ &\times \frac{(1-\exp\lambda[1-(1+x^{\beta})^{k}])^{\alpha-1}}{(1+x^{\beta})^{-k+1}(1+\exp\lambda[1-(1+x^{\beta})^{k}])^{\alpha+1}}, \end{aligned}$$

  where $\alpha,\lambda,\beta,k>0$, and $x>0$.
- Kumaraswamy Weibull distribution (KW) [20] with the pdf

$$f_{KW}(x;a,b,\alpha,\beta) = ab\alpha^{\beta}x^{\beta-1}\exp\left(-\alpha x^{\beta}\right)\left(1-\exp\left(-\alpha x^{\beta}\right)\right)^{a-1}\left[1-\left(1-\exp-(\alpha x)^{\beta}\right)^{a}\right]^{b-1},$$

  where $a,b,\alpha,\beta>0$, and $x>0$.
- The Topp-Leone type I heavy-tail log-logistic Poisson (TL-HT-LLOGP) [6] with the pdf

$$\begin{aligned} f_{TL-HT-LLOGP}(x;b,\theta,\delta,\beta) &= 2b\delta^{2}\theta\left[1-\left(\frac{1}{[1+x^{\beta}](1-(1-\delta)(1-[1+x^{\beta}]^{-1}))}\right)^{2\delta}\right]^{b-1} \\ &\times \frac{\beta x^{\beta-1}[1+x^{\beta}]^{-2}\left[(1+x^{\beta})^{-1}\right]^{2\delta-1}}{\left[1-(1-\delta)(1-[1+x^{\beta}]^{-1})\right]^{2\delta+1}} \\ &\times \frac{\exp\left(\theta\left(1-\left(1-\left[\frac{[1+x^{\beta}]^{-1}}{1-(1-\delta)(1-[1+x^{\beta}]^{-1})}\right]^{2\delta}\right)^{b}\right)\right)}{\exp(\theta)-1}, \end{aligned}$$

  where $b,\theta,\delta,b>0$.

- The exponentiated half logistic odd Burr III log-logistic (EHL-OBIII-LLoG) [21] with pdf

$$\begin{aligned} f_{EHL-OBIII-LLoG}(x;a,b,\alpha,c) &= 2\alpha ab\left(\left(1+\left(\frac{1-(1+x^{\lambda})^{-1}}{(1+x^{\lambda})^{-1}}\right)^{-\alpha}\right)^{-b}\right)^{\alpha-1}\left(1+\left(\frac{1-(1+x^{\lambda})^{-1}}{(1+x^{\lambda})^{-1}}\right)^{-\alpha}\right)^{-b-1} \\ &\times \left(1+\left[1-\left(1+\left(\frac{1-(1+x^{\lambda})^{-1}}{(1+x^{\lambda})^{-1}}\right)^{-\alpha}\right)^{-b}\right]\right)^{-(\alpha+1)} \\ &\times \left(\frac{1-(1+x^{\lambda})^{-1}}{(1+x^{\lambda})^{-1}}\right)^{-\alpha-1}\frac{\lambda x^{\lambda-1}(1+x^{\lambda})^{-2}}{\left((1+x^{\lambda})^{-1}\right)^{2}}, \end{aligned}$$

  where $\alpha, a, b, \lambda > 0$.

The comparative performance of the candidate models is evaluated using a suite of six goodness-of-fit (GoF) measures. The foundational measure is the log-likelihood value, -2log(L), which quantifies the overall fit to the data. To account for model parsimony and to mitigate overfitting, we employ four information criteria that penalize model complexity: the Akaike Information Criterion (AIC), the Bayesian Information Criterion (BIC), the Consistent Akaike Information Criterion (CAIC) with its more severe penalty, and the Hannan-Quinn Criterion (HQIC), which seeks a balance between the consistency of the BIC and finite-sample performance. Finally, the Kolmogorov-Smirnov (K-S) test statistic and its associated p-value are used to assess the distributional adequacy by measuring the supremum distance between the empirical and the modeled cumulative distribution functions. To estimate the parameters of the HT-WF-BXII model, the non-linear minimization function (nlm) in the R software was utilized. Parameter estimates accompanied by their respective standard errors (SEs), are indicated within the parentheses. To verify the identifiability of the parameter estimates, profile log-likelihood plots were constructed for all analyzed datasets. The model validation was further supported through multi-faceted graphical diagnostics, including the following: (i) fitted probability density curves, (ii) probability-probability (P-P) plots with sum of squares in parentheses, (iii) empirical cumulative distribution functions (ECDFs), (iv) Kaplan-Meier (K-M) survival curves, (v) scaled total time on test (TTT) transformations, and (vi) hrf plots.

7.1. Lung cancer data

This dataset presents information on advanced lung cancer patients sourced from a study referenced in [22]. These patients were randomly allocated to receive standard chemotherapy treatments. The survival times (t) were recorded from the initiation of treatment for each individual in the study. The dataset is as follows: 411, 126, 118, 82, 8, 25, 11, 54, 153, 16, 56, 21, 287, 10, 8, 12, 177, 12, 200, 250, and 100.

The MLEs along with their corresponding SEs (shown in parentheses) are displayed in Table 3. The GoF results from Table 3 show that the HT-WF-BXII model fits the data better compared to its competitors. The 95% asymptotic confidence intervals (ACI) for the parameters of the HT-WF-BXII distribution are as follows: $\alpha \in (1.6311 \pm 0.6138)$, $\lambda \in (1.0025 \pm 0.4220)$, $\beta \in (5.9767 \pm 5.02 \times 10^{-5})$, and $k \in (0.0402 \pm 8.84 \times 10^{-3})$. The parameters of the HT-WF-BXII model on lung cancer data are uniquely identifiable, as depicted in Figure 7.

Table 3. Lung cancer data: Parameter estimates and GoF statistics.

	Estimates				Statistics						
Distribution	α	λ	β	k	-2log(L)	AIC	CAIC	BIC	$HQIC$	K−S	p−value
HT-WF-BXII	1.6311	1.0025	5.9767	0.0402	233.6525	241.6525	244.1525	245.8306	242.5593	0.1491	0.7387
	(0.3132)	(0.2153)	(2.56×10^{-5})	(4.51×10^{-3})							
	α	β	b	λ							
TL-OBIII-LLOG	11.4267	133.8261	0.1194	0.0693	234.8169	242.8169	245.3169	246.9950	243.7237	0.1511	0.7132
	(7.2144)	(0.0280)	(0.0418)	(0.0438)							
	α	λ	γ	−							
TIHT-W	0.9215	1.3118	9.63×10^{-3}	-	235.9407	241.9407	244.8525	245.9743	242.8208	0.1595	0.6591
	(0.1961)	(1.1740)	(0.0215)	(-)							
	α	λ	β	k							
OEHL-BXII	10.0000	1.46×10^{-3}	0.0267	10.1260	326.3061	334.3061	336.8051	338.4832	335.2118	0.3703	0.0630
	(1.56×10^{-3})	(2.07×10^{-4})	(5.22×10^{-3})	(2.81×10^{-6})							
	a	b	α	β							
KW	50.9190	19.1150	111.1900	0.0920	235.1406	243.1406	245.6406	247.3187	244.0473	0.1502	0.7006
	(11.6710)	(3.6689)	(0.0729)	(5.07×10^{-3})							
	b	θ	δ	β							
TL-HT-LLOGP	7.6990	2.18×10^{-5}	0.1316	3.0045	235.6267	243.6267	246.1267	247.8084	244.5335	0.1673	0.5993
	(4.5911)	(0.0176)	(0.1274)	(2.8052)							
	a	b	α	c							
EHL-OBIII-LLOG	222.4700	0.0575	166.8700	4.01×10^{-3}	236.0474	244.0474	246.5474	248.2255	244.9542	0.1647	0.6189
	(1.18×10^{-3})	(0.0256)	(8.88×10^{-6})	(6.57×10^{-4})							

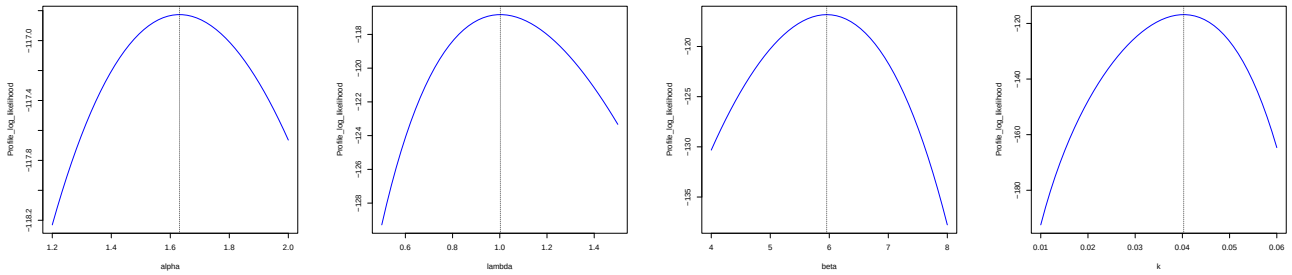

(a) **(b)** **(c)** **(d)**

Figure 7. Profile log-likelihood plots for lung cancer data.

The plots illustrated in Figure 8 indicate that the HT-WF-BXII distribution demonstrates a superior performance compared to the non-nested models when applied to the lung cancer data. The graphical representation depicted in Figure 9 illustrates the observed and fitted ECDF as well as the K-M survival curves for the lung cancer data. The plots demonstrate that the HT-WF-BXII distribution closely aligns with the observed ECDF and K-M survival curves.

Figure 10 exhibits the TTT scaled plot and HRF plots, which reveal an inverted bathtub-shaped hazard rate pattern for the lung cancer data.

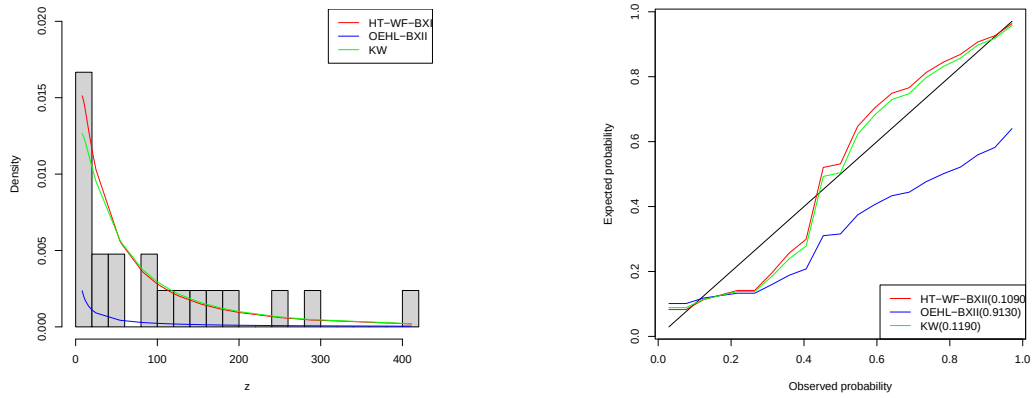

Figure 8. Graphical representations of the fitted density functions and probability plots for the lung cancer data.

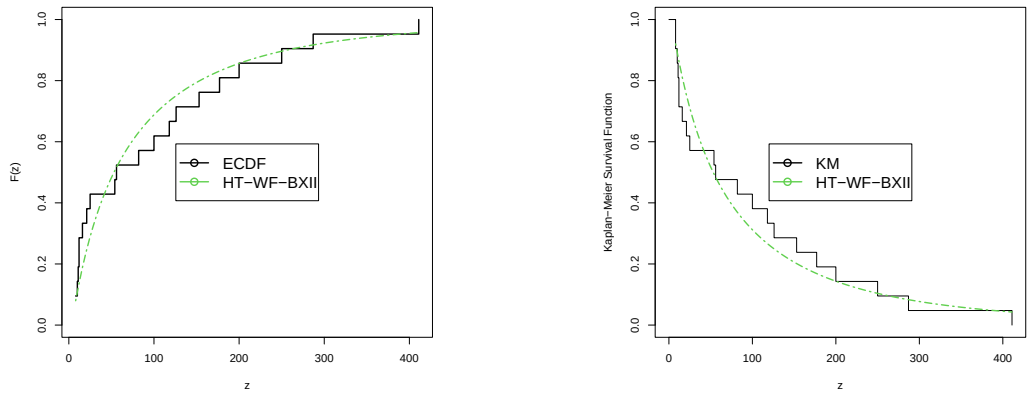

Figure 9. Fitted ECDF curve and K-M plots for for lung cancer data.

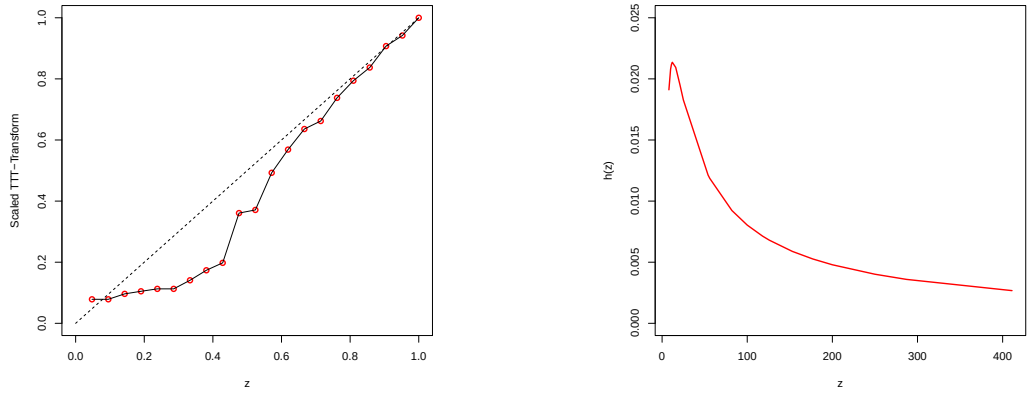

Figure 10. Fitted TTT scaled and hrf plots for the lung cancer data.

7.2. Acute myeloid leukemia data

This dataset contains the survival times in months of 20 patients with acute myeloid leukemia (a rapid cancer of the bone marrow that crowds out healthy blood cells). The dataset was previously analyzed by [23, 24]. The values are as follows: 2.226, 2.113, 3.631, 2.473, 2.720, 2.050, 2.061, 3.915, 0.871, 1.548, 2.746, 1.972, 2.265, 1.200, 2.967, 2.808, 1.079, 2.353, 0.726, and 1.958.

The MLEs along with their corresponding SEs (shown in parentheses) are displayed in Table 4. The GoF results show that the HT-WF-BXII model fits the data better compared to its competitors. The 95% asymptotic confidence intervals (ACI) for the parameters of the HT-WF-BXII distribution are as follows: $\alpha \in (8.2750 \pm 5.19 \times 10^{-3})$, $\lambda \in (0.9946 \pm 0.4334)$, $\beta \in (0.2368 \pm 0.0895)$, and $k \in (1.3183 \pm 0.1121)$. The parameters of the HT-WF-BXII model on myeloid leukemia data are uniquely identifiable, as depicted in Figure 11.

Table 4. Acute myeloid leukemia data: parameter estimates and GoF statistics.

	Estimates				Statistics						
Distribution	α	λ	β	k	-2log(L)	AIC	CAIC	BIC	$HQIC$	K−S	p−value
HT-WF-BXII	8.2750	0.9946	0.2368	1.3183	48.2333	56.2333	58.9199	60.2362	57.0308	0.1541	0.6732
	(2.65×10^{-3})	(0.2211)	(0.0457)	(0.0572)							
	α	β	b	λ							
TL-OBIII-LLOG	11.0810	12.5170	0.3497	0.1932	53.2611	61.2611	63.9277	65.2440	62.0386	0.2456	0.1508
	(7.17×10^{-4})	(16.8420)	(0.5178)	(0.0409)							
	α	λ	γ	−							
TIHT-W	1.3672	9.8532	3.49×10^{-3}	-	62.7417	68.7417	70.2417	71.7289	69.3248	0.3086	0.0644
	(0.2794)	(4.46×10^{-4})	(1.18×10^{-3})	(-)							
	α	λ	β	k							
OEHL-BXII	0.1680	3.39×10^{-5}	26.6950	0.3140	52.2334	60.2334	62.9000	64.2163	61.0109	0.1744	0.5209
	(0.0318)	(2.19×10^{-5})	(2.14×10^{-4})	(0.0162)							
	a	b	α	β							
KW	50.5036	110.8538	0.0807	5.7756	48.2493	56.2493	58.8160	60.2223	57.0468	0.1548	0.6585
	(3.9098)	(0.1663)	(0.0218)	(44.8134)							
	b	θ	δ	β							
TL-HT-LLOGP	0.5457	153.4800	5.92×10^{-4}	5.6374	48.5601	56.5601	59.2268	60.5431	57.3377	0.1597	0.6305
	(0.1171)	(2.11×10^{-6})	(5.93×10^{-4})	(0.0104)							
	a	b	α	c							
EHL-OBIII-LLOG	222.4800	0.0119	166.8100	0.0112	55.9179	63.9179	66.5846	67.9009	64.6954	0.2556	0.1221
	(8.33×10^{-8})	(2.87×10^{-3})	(2.06×10^{-7})	(1.66×10^{-3})							

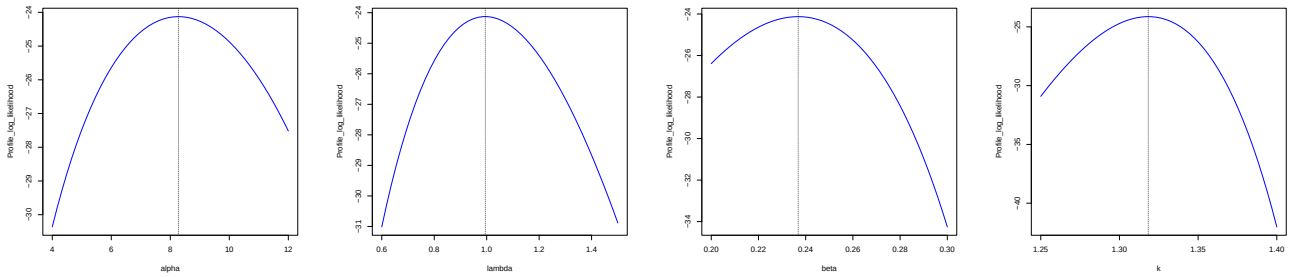

(a) **(b)** **(c)** **(d)**

Figure 11. Profile log-likelihood plots for the myeloid leukemia data.

The plots illustrated in Figure 12 indicate that the HT-WF-BXII distribution demonstrates superior performance compared to the non-nested models when applied to the myeloid leukemia data. The graphical representation depicted in Figure 13 illustrates the observed and fitted ECDF as well as the K-M survival curves for the myeloid leukemia data. The plots demonstrate that the HT-WF-BXII distribution closely aligns with the observed ECDF and K-M survival curves.

Figure 14 exhibits the TTT scaled plot and HRF plots, which reveal an increasing hazard rate pattern for the myeloid leukemia data.

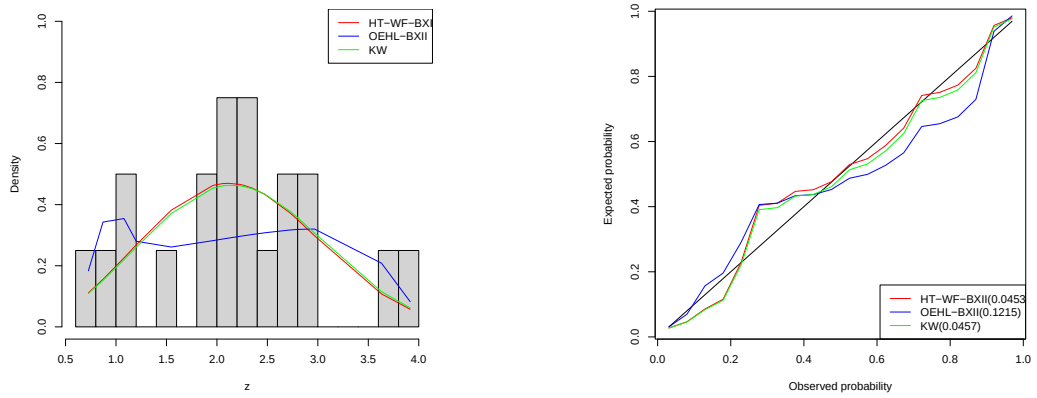

Figure 12. Graphical representations of the fitted density functions and probability plots for the myeloid leukemia data.

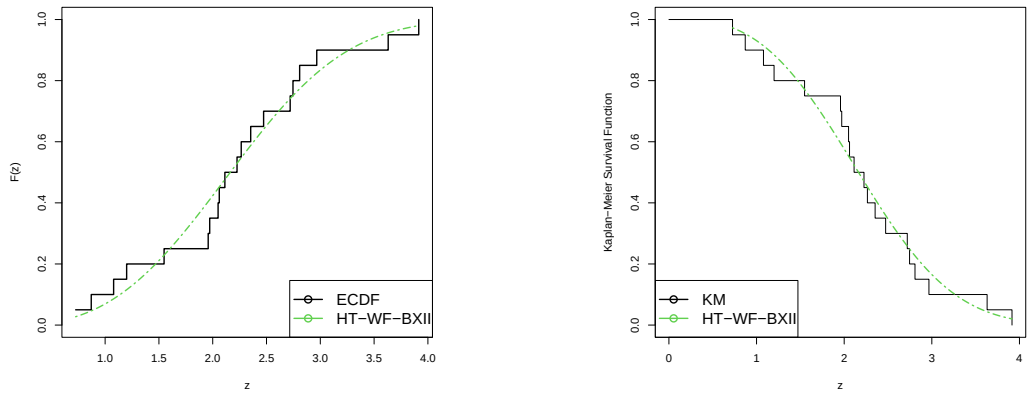

Figure 13. Fitted ECDF curve and K-M plots for the myeloid leukemia data.

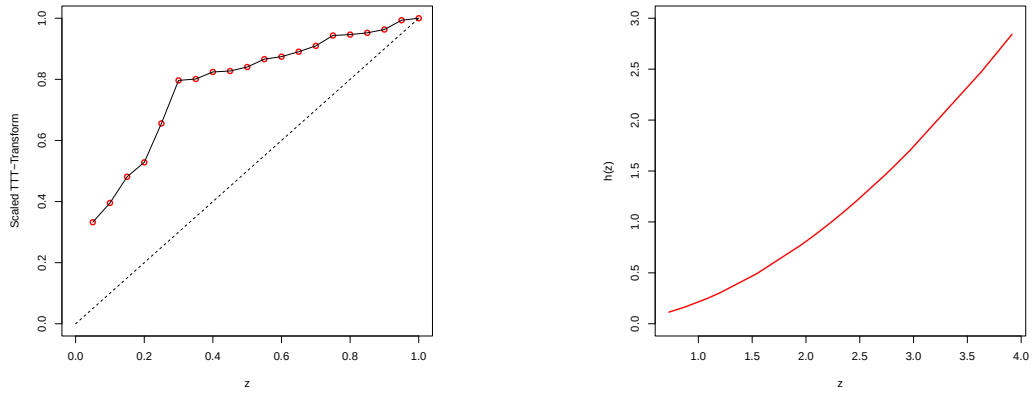

Figure 14. Fitted TTT scaled and hrf plots for the myeloid leukemia data.

8. Conclusions and recommendations

This paper introduced the HT-WF-G family of distributions, a robust and highly flexible probability framework designed to model complex real-world phenomena characterized by heavy tails, skewness, and non-monotonic hazard rates. By integrating the heavy-tailed-G generator with the Weibull flexible-G baseline, the proposed family significantly extends the capability to capture diverse data behaviors that traditional distributions often fail to adequately model. Through rigorous theoretical development, we derived the fundamental statistical properties of the HT-WF-G family, including its quantile function, series expansion, and moments.

The MLE procedure was established and validated via comprehensive Monte Carlo simulations, thus confirming the consistency and efficiency of the parameter estimates. The formulation of key actuarial risk measures within this framework enhances its applicability in financial and insurance risk assessments. The practical superiority of the HT-WF-G family, particularly its HT-WF-BXII special case, was decisively demonstrated through applications in oncology. Using time-to-event data for lung cancer and acute myeloid leukemia, the model consistently outperformed several prominent

benchmark distributions across multiple GoF criteria, including AIC, BIC, CAIC, HQIC, and the K-S test. This empirical validation underscores the model's utility as a statistical tool for survival analyses and reliability engineering in heavy-tailed and complex settings.

While the HT-WF-G family demonstrated an enhanced flexibility and superior fit in the analyzed oncology datasets, its increased parametric complexity raises concerns regarding overfitting, particularly with limited samples. Furthermore, the presence of extremely small standard errors for some parameters may indicate numerical rather than substantive precision. Moreover, the model's current formulation does not accommodate censored observations—a common feature in survival data—potentially biasing the estimates. Future work should address these limitations by incorporating regularization or penalized estimations, validating results via bootstrap and sensitivity analyses, extending the framework to handle censoring, and assessing the predictive performance through cross-validation and simulations under realistic conditions. Developing bivariate or multivariate versions of the HT-WF-G family using copula functions or other multivariate construction methods would allow for the modeling of complex dependence structures between random variables, with direct applications in finance, insurance, and multi-state survival analyses. Furthermore, applying the HT-WF-G family to other domains with heavy-tailed and skewed data, such as climatology (extreme weather events), econometrics (financial returns), and actuarial science (catastrophic loss modelling), would further demonstrate its versatility and practical impact.

The HT-WF-G family, with its demonstrated flexibility and superior fit, establishes a substantive foundation for advanced statistical modeling. Pursuing these future directions will not only extend the theoretical reach of the family but also broaden its scope to solve complex analytical problems across diverse scientific and industrial fields.

Author contributions

Conceptualization, F. Chipepa and W. Nkomo; Methodology, F. Chipepa, W. Nkomo and M. M. Hasaballah.; Software, W. Nkomo and M. M. Abdelwahab; Validation, M. M. Abdelwahab; Formal analysis, M. M. Hasaballah and M. M. Abdelwahab; Investigation, F. Chipepa and M. M. Hasaballah; Data curation, M. M. Hasaballah; Writing—original draft, F. Chipepa. and W. Nkomo; Writing—review & editing, M. M. Hasaballah and M. M. Abdelwahab; Visualization, M. M. Abdelwahab; Funding acquisition, M. M. Hasaballah. All authors have read and agreed to the published version of the manuscript.

Use of Generative-AI tools declaration

The authors declare that they have not used Artificial Intelligence (AI) tools in the creation of this article.

Data availability

The original contributions presented in this study are included in the article. Further inquiries can be directed to the corresponding author.

Conflict of interest

The authors declare no conflicts of interest.

References

1. A. Alzaatreh, C. Lee, F. Famoye, A new method for generating families of continuous distributions, *Metron*, **71** (2013), 63–79. https://doi.org/10.1007/s40300-013-0007-y
2. M. H. Tahir, M. Zubair, M. Mansoor, G. M. Cordeiro, M. Alizadeh, G. G. Hamedani, A new Weibull-G family of distributions, *Hacettepe J. Math. Stat.*, **45** (2016), 629–647.
3. G. M. Cordeiro, M. Alizadeh, E. M. Ortega, The expo- nentiated half-logistic family of distributions: properties and applications, *J. Probab. Stat.*, **4** (2014), 864396. https://doi.org/10.1155/2014/864396
4. W. Zhao, S. K. Khosa, Z. Ahmad, M. Aslam, A. Z. Afify, Type-I heavy tailed family with applications in medicine, engineering and insurance, *PloS One*, **15** (2020), e0237462. https://doi.org/10.1371/journal.pone.0237462
5. J. Zhao, Z. Ahmad, E. Mahmoudi, E. H. Hafez, M. M. Mohie El-Din, A new class of heavy-tailed distributions: modeling and simulating actuarial measures, *Complexity*, **2021** (2021), 5580228. https://doi.org/10.1155/2021/5580228
6. W. Nkomo, B. Oluyede, F. Chipepa, Topp-Leone type I heavy-tailed-G power series class of distributions: properties, risk measures, and applications, *Stat., Optim. Inf. Comput.*, **13** (2025), 88–110. https://doi.org/10.19139/soic-2310-5070-2039
7. A. Z. Afify, A. M. Gemeay, N. A. Ibrahim, The heavy-tailed exponential distribution: risk measures, estimation, and application to actuarial data, *Mathematics*, **8** (2020), 1–28. https://doi.org/10.3390/math8081276
8. A. A. M. Teamah, A. A. Elbanna, A. M. Gemeay, Heavy-tailed log-logistic distribution: Properties, risk measures and applications, *Stat., Optim. Inf. Comput.*, **9** (2021), 910–941. https://doi.org/10.19139/soic-2310-5070-1220
9. T. Moakofi, B. Oluyede, The type I heavy-tailed odd power generalized Weibull-G family of distributions with applications, *Commun. Fac. Sci. Univ. Ankara Ser. A1 Math. Stat.*, **72** (2023), 921–958. https://doi.org/10.31801/cfsuasmas.1195058
10. M. Gwazane, B. Oluyede, F. Chipepa, The new family of exponentiated half logistic-type I heavy-tailed-G distributions with applications, *Electron. J. Appl. Stat. Anal.*, **18** (2025), 102–132. https://doi.org/10.1285/i20705948v18n1p102
11. G. Warahena-Liyanage, B. Oluyede, T. Moakofi, The new Ristić-Balakrishnan-heavy-tailed-type II Topp-Leone-G family of distributions with ap- plications, *J. Stat. Theory Appl.*, **24** (2025), 354–393. https://doi.org/10.1007/s44199-025-00113-2
12. W. Nkomo, B. Oluyede, F. Chipepa, Type I heavy-tailed family of generalized Burr III distributions: properties, actuarial measures, regression and applications, *Stat. Transition New Ser.*, **26** (2025), 93–115. https://doi.org/10.59139/stattrans-2025-006

13. G. M. Cordeiro, E. C. Biazatti, E. M. M Ortega, M. de Lima, S. D. Carmo, L. H. De Santana, The Weibull flexible generalized family of bimodal distributions: properties, simulation, regression models, and applications, *Chilean J. Stat.*, **15** (2024), 27–43. https://doi.org/10.32372/ChJS.15-01-02
14. M. H. Tahir, M. A. Hussain, G. M. Cordeiro, A new flexible generalized family for constructing many families of distributions, *J. Appl. Stat.*, **49** (2022), 1615–1635. https://doi.org/10.1080/02664763.2021.1874891
15. M. Bourguignon, R. B. Silva, G. M. Cordeiro, The Weibull-G family of probability distributions, *J. Data Sci.*, **12** (2014), 53–68.
16. I. W. Burr, Cumulative frequency functions, *Ann. Math. Statist.*, **13** (1942), 215–232. https://doi.org/10.1214/aoms/1177731607
17. A. Henningsen, O. Toomet, maxLik: A package for maximum likelihood estima- tion in R, *Comput. Stat.*, **26** (2011), 443–458. https://doi.org/10.1007/s00180-010-0217-1
18. M. Aldahlan, A. Z. Afify, The odd exponentiated half-logistic Burr XII distribution, *Pak. J. Stat. Oper. Res.*, **14** (2018), 305–317. https://doi.org/10.18187/pjsor.v14i2.2285
19. T. Moakofi, B. Oluyede, M. Gabanakgosi, The Topp-Leone odd Burr III-G family of distributions: model, properties and applications, *Stat., Optim. Inf. Comput.*, **10** (2022), 236–262. https://doi.org/10.19139/soic-2310-5070-1135
20. G. M. Cordeiro, E. M. M. Ortega, S. Nadarajah, The Kumaraswamy Weibull distribution with application to failure data, *J. Franklin Inst.*, **347** (2010), 1399–1429. https://doi.org/10.1016/j.jfranklin.2010.06.010
21. B. Oluyede, P. O. Peter, N. Ndwapi, H. Bindele, The exponentiated half-logistic odd Burr III-G: model, properties and applications, *Pak. J. Stat. Oper. Res.*, **18** (2022), 33–57. https://doi.org/10.18187/pjsor.v18i1.3668
22. E. T. Lee, J. Wang, *Statistical methods for survival data analysis*, 2 Eds., John Wiley & Sons, 2003. https://doi.org/10.1002/0471458546
23. A. Z. Afify, Z. M. Nofal, N. S. Butt, Transmuted complementary Weibull geometric distribution, *Pak. J. Stat. Oper. Res.*, **10** (2014), 435–454. https://doi.org/10.18187/pjsor.v10i4.836
24. D. N. P. Murthy, M. Xie, R. Jiang, *Weibull models*, John Wiley & Sons, 2004. http://dx.doi.org/10.1002/047147326X

AIMS Press